Planta (2018) 247:393–404
https://doi.org/10.1007/s00425-017-2793-6

ORIGINAL ARTICLE

The *Ceratopteris* (fern) developing motile gamete walls contain diverse polysaccharides, but not pectin

Renee A. Lopez[1] · **Karen S. Renzaglia**[1]

Received: 20 July 2017 / Accepted: 5 October 2017 / Published online: 13 October 2017

Abstract
Main conclusion **Unlike most plant cell walls, the five consecutive walls laid down during spermatogenesis in the model fern *Ceratopteris* contain sparse cellulose, lack pectin and are enriched with callose and hemicelluloses.**

Seed-free plants like bryophytes and pteridophytes produce swimming male gametes for sexual reproduction. During spermatogenesis, unique walls are formed that are essential to the appropriate development and maturation of the motile gametes. Other than the detection of callose and general wall polysaccharides in scattered groups, little is known about the sequence of wall formation and the composition of these walls during sperm cell differentiation in plants that produce swimming sperm. Using histochemistry and immunogold localizations, we examined the distribution of callose, cellulose, mannan and xylan-containing hemicelluloses, and homogalacturonan (HG) pectins in the special walls deposited during spermatogenesis in *Ceratopteris*. Five walls are produced in sequence and each has a unique fate. The first wall (W1) contains callose and sparse xylan-containing hemicelluloses. Wall two (W2) is thin and composed of cellulose crosslinked by xylan-containing hemicelluloses. The third wall (W3) is thick and composed entirely of callose, and the fourth wall (W4) is built of cellulose heavily crosslinked by galactoxyloglucan hemicelluloses. Wall five (W5) is an arabinogalactan protein (AGP)-rich matrix in which the gamete changes shape and multiple flagella elongate. We detected no esterified or unesterified HG pectins in any of the walls laid down during spermatogenesis. To consider evolutionary modifications in cell walls associated with motile gametes, comparisons are presented with male gametophyte and spermatogenous cell walls across plant groups.

Keywords Callose · Cell walls · Galactoxyloglucans · Hemicelluloses · Pectins · Spermatogenesis · Xyloglucans

Abbreviations

AGP	Arabinogalactan proteins
ßGlucY	ß-D-glucosyl Yariv
HG	Homogalacturonan
MAb	Monoclonal antibodies

Introduction

Cell walls in plants are living "cages" around protoplasts that manage tensile and compressive forces, regulate cell expansion and adhesion and are the foundation of differentiation into specific cell types (Evert 2006; Knox 2008; Burgert and Fratzl 2009). Cell walls play important roles during sexual reproduction in seed plants by protecting vulnerable cells from desiccation (Herburger et al. 2015) and pathogen attack (Jacobs et al. 2003; Nishimura et al. 2003; Ton and Mauch-Mani 2004; Flors et al. 2005; El Hadrami et al. 2010; Luna et al. 2011), delivering signals (Buchanan et al. 2000; McCabe et al. 1997; Wolf et al. 2012) and transporting sperm cells to the egg (Rudall and Bateman 2007). In seed-free plants (bryophytes and pteridophytes), unique walls are formed during spermatogenesis that are integral to the proper development and maturation of the motile gametes (Cave and Bell 1973; Gorska-Brylass 1969; Kotenko

✉ Renee A. Lopez
rlopezswalls@gmail.com; ralopez@siu.edu

[1] Department of Plant Biology, MC:6509, Southern Illinois University Carbondale, Carbondale, IL 62901, USA

1990; Kaźmierczak 2008; Muccifora and Bellani 2011; Lopez and Renzaglia 2014).

Spermatogenesis is a complicated process in archegoniates as it involves the complete transformation of every cellular component into a coiled flagellated cell that is devoid of a cell wall at maturity (Renzaglia and Garbary 2001). Other than the detection of callose and general wall polysaccharides in scattered groups, little is known about the sequence of wall formation and the composition of these walls during sperm cell differentiation in seed-free plants (Gorska-Brylass 1969; Cave and Bell 1973; Kámeiczak 2008; Muccifora and Bellani 2011). Using immunogold localization, we reported the differential expression of AGP epitopes in the matrix surrounding spermatids of the leptosporangiate fern *Ceratopteris* (Lopez and Renzaglia 2014). The abundance of AGPs as flagella grow and the cell assumes a coiled configuration is consistent with the speculated regulation of these glycoproteins in Ca^{+2} signaling necessary for cytomorphogenesis (Lamport and Varney 2013). However, the polysaccharide composition, structure and function of the series of special walls during spermatogenesis have not been explored in any plant that produces swimming sperm.

In this investigation, we present a complete study of the microanatomy and polysaccharide constituents of the special walls deposited during spermatogenesis in *Ceratopteris.* Beginning with antheridial development, we follow the development of four consecutive special walls (W1–W4) up to and including the deposition of the AGP-enriched extraprotoplasmic matrix (W5) described in Lopez and Renzaglia (2014). Each wall was probed with histochemical stains in the light and fluorescence microscope, and eight monoclonal antibodies (MAbs) raised against pectins, cellulose, hemicelluloses and callose in the transmission electron microscope. All five walls differ markedly from the typical primary wall of parenchyma cells and each has a unique fate. The functions of these walls are considered based on polymer composition. To consider evolutionary modifications in cell walls associated with motile gametes, comparisons are presented with male gametophyte and spermatogenous cell walls across plant groups.

Materials and methods

Gametophyte culture

Male gametophytes of *Ceratopteris richardii* were grown from spores (*him1* "mostly male" mutant strain) and sown on Parker medium with Thompson micronutrients per the sterile culture techniques outlined by Warne et al. (1986). Cultures were maintained at 28 °C under continuous light. The *him1* mutant strain that forms only male gametophytes and not hermaphrodites was used to ensure ample antheridia for observation.

Specimen preparation for transmission electron microscopy

Male gametophytes were fixed in 2% v/v glutaraldehyde in 0.05 M Na2HPO4 (pH 7.2), post-fixed 1% (w/v) OsO4 (15 min), dehydrated and embedded in LR White resin (London Resin Company, Berkshire, UK) as described in Lopez and Renzaglia (2014). Thin sections were collected on nickel grids and post-stained with uranyl acetate (3 min) and Reynolds lead citrate (30 s). Samples were viewed and micrographs were digitally collected in a Hitachi H7650.

Histochemical staining

Callose was detected in antheridia of whole-mount male gametophytes incubated for 24 h in 1% aniline blue in 0.067 M Na2HPO4 (pH 8.5) buffer in the dark followed by several rinses in the same buffer. To visualize cellulose/hemicellulose, whole mounts and resin-embedded thick sections (1 µm) were placed on glass slides with a drop of calcofluor white (Sigma-Aldrich) stain and a drop of 10% potassium hydroxide for 3 min. All stained materials were viewed under a Leica DM5000 B compound microscope using UV fluorescence. Controls were made using the respective buffers without aniline blue or calcofluor white.

Yariv staining for AGPs

The Yariv reagent, ß-D-glucosyl (ßGlucY), is a red stain used to detect plant AGPs (Yariv et al. 1967). Whole-mount gametophytes grown for 14 d in sterile culture (on Parker–Thompson medium at 28 °C under continuous light) were incubated for 18 h in ßGlucY (1000 µm) followed by three rinses in 0.15 M NaCl buffer. Stained materials were viewed and imaged using a Leica DM5000 B compound microscope equipped with DIC optics (differential interference contrast). Yariv reagents were purchased from Biosupplies Australia Pty (Victoria, Australia).

Immunogold labeling for cell wall constituents

Eight primary monoclonal antibodies (MAbs) were used to detect cellulose (CBM3a), 1,3-β-glucan (anti-callose), xyloglucans (LM15), mannans (LM21), galactoxyloglucans (LM25), glucuronoxylans (LM28), unesterified homogalacturonan (HG) pectins (LM19) and esterified HG pectins (LM20) (Table 1). Controls grids were prepared by excluding the primary antibodies. The grids were processed for TEM as described in Lopez and Renzaglia (2014).

Table 1 Monoclonal primary antibodies used for immunolocalizations of cell wall compounds during spermatogenesis in *Ceratopteris richardii*

Antibody	Antigen (s)/epitope	Reference/source
CBM3a	Crystalline cellulose	Blake et al. 2006/J. P. Knox PlantProbes, University of Leeds, UK
Anti-callose	Callose/(1,3)-β-linked penta- to hexaglucan	Meikle et al. 1991/Biosupplies Australia
LM15	XXXG motif of xyloglucan	Marcus et al. 2008/J. P. Knox PlantProbes, University of Leeds, UK
LM21	Mannan/β-(1,4)-manno-oligosaccharide	Marcus et al. 2010/J. P. Knox PlantProbes, University of Leeds, UK
LM25	Galactosylated xyloglucans	Pedersen et al. 2012/J. P. Knox PlantProbes, University of Leeds, UK
LM28	Glucuronoxylan	Cornuault et al. 2015/J. P. Knox PlantProbes, University of Leeds, UK
LM19	Homogalacturonan/methyl-esterified	Verhertbruggen et al. 2009/J. P. Knox PlantProbes, University of Leeds, UK
LM20	Homogalacturonan/unesterified	Verhertbruggen et al. 2009/J. P. Knox PlantProbes, University of Leeds, UK

Results

There are five consecutive walls produced during spermatogenesis in *Ceratopteris richardii*. As depicted in Fig. 1, these walls begin with the primary walls that delineate spermatogenous cells in the young antheridium and end with the extraprotoplasmic matrix in which sperm cells differentiate.

Antheridia of *Ceratopteris richardii* consist of three sterile jacket cells (a cap cell and two ring cells) that surround the spermatogenous tissue (Fig. 2a). A single spermatogenous cell, the primary androgone, is delimited in the nascent antheridium, and it undergoes five synchronized mitotic divisions to produce 32 spermatids (immature gametes). Spermatogenous cells contain dense cytoplasm with large central nuclei and elongated, dense plastids with few thylakoids and scattered starch (Fig. 2b). Cells are polygonal and surrounded by thin walls (W1) that are primarily composed of callose as evidenced by aniline blue fluorescence (Fig. 2c) and strong labeling with the anti-callose MAb (Fig. 2d). Calcofluor white staining gives a faint fluorescence indicating the presence of cellulose/hemicellulose in the walls between jacket and spermatogenous tissue, but not in the thin walls of the spermatogenous cells (Fig. 2e). The walls of the antheridium and surrounding vegetative cells took on the calcofluor stain intensely. Corroborating this finding is that immunogold labeling of spermatogenous cell walls with the CBM3a MAb shows a very weak and uneven binding pattern supporting the scarcity of cellulose (Fig. 2f).

Two xylose-containing hemicellulose epitopes are expressed in the first walls (W1) in spermatogenous cells,

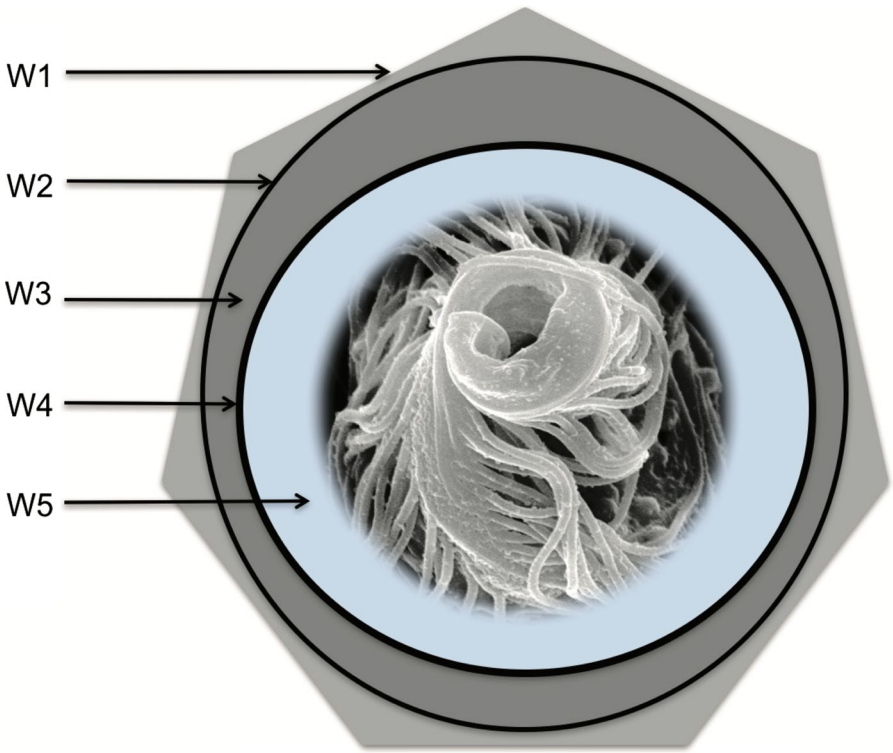

Fig. 1 Diagram illustrating the five walls (W1–W5) deposited during spermatogenesis in *Ceratopteris richardii*. W1 separates the rapidly dividing spermatogenous cells. W2–W5 are laid down in sequence by the developing spermatid

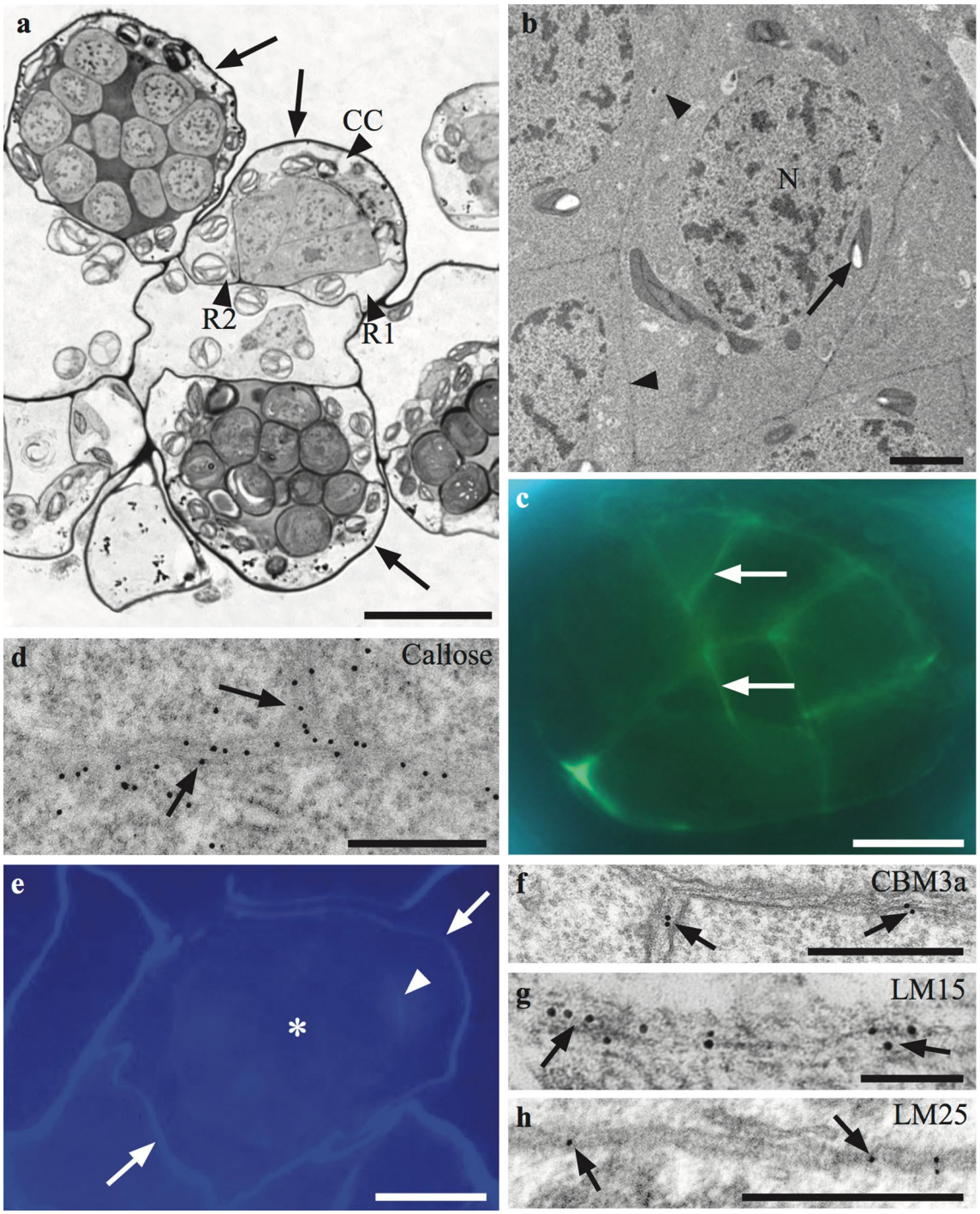

Fig. 2 Spermatogenous cell walls (W1) of *Ceratopteris richardii*. **a** Light micrograph of a male gametophyte with antheridia (*arrows*). Each antheridium is composed of two ring cells (*R1, R2*) and a cap cell (*CC*) and contains spermatogenous (*upper middle*) and spermatids at different stages of development. **b** Transmission electron micrograph (TEM) of polygonal spermatogenous cells surrounded by thin cell walls (W1) (*arrowheads*). Each has a large central nucleus (*N*) surrounded by plastids, some containing single starch grains (*arrow*). **c** Walls of spermatogenous cells (*arrows*) fluoresce brightly with aniline blue illustrating the abundance of callose. **d** TEM of spermatogenous walls showing abundant immunogold labels bound to callose epitopes (*arrows*). **e** Calcofluor white staining of a section of an antheridium containing four spermatogenous cells (*asterisk*). Only jacket cell (*arrowhead*) and vegetative cell walls (*arrows*) fluoresce brightly, indicating that very little cellulose occurs in spermatogenous cell walls. **f** TEM of spermatogenous walls that label weakly or not at all with CMB3a for cellulose (*arrows*). **g**, **h** Immunogold labeling of hemicelluloses. **g** Xyloglucan epitopes (LM15 MaAb) are present in spermatogenous cell walls (*arrows*) with more abundance compared to the galactoxyloglucan epitopes (*arrows*) labeled with the LM25 MAb in **h**. *Scale bars*: 20 µm for **a**; 2 µm for **b**; 10 µm for **c**; 500 nm **d**; 10 µm for **e**; 500 nm for **f**–**h**

with xyloglucan (labeled with LM15) more abundant (Fig. 2g) than galactoxyloglucan (labeled with LM25) (Fig. 2h). Glucuronoxylan and mannan epitopes were not detected in W1 with the LM28 and LM21 MAbs, respectively (data not shown).

Regarding pectins in W1, unesterified HG epitopes (LM19 MAb) were not detected during cell plate formation in dividing spermatogenous cells (Fig. 3a), and methyl-esterified HG epitopes (LM20 MAb) were not detected in the thin spermatogenous walls (Fig. 3b). In contrast, these pectin epitopes (LM19, Fig. 3c) (LM20, Fig. 3d) are relatively abundant in the antheridial walls.

Spermatids build a series of unique walls or matrices (W2–W5) that are associated with the stages of sperm cell differentiation. As the final mitotic division is giving rise to male gametes (Fig. 4a), callose rapidly disappears and faint calcofluor-binding polymers appear for the first time in the thin rounded walls (W2) of the nascent spermatids (Fig. 4b). Following deposition of W2, a thick callosic wall (W3) is unevenly deposited and further separates the rounded spermatid from the primary cell walls (W1 and W2) (Fig. 4c). Callose deposition is thickest (approximately 1.6 µm) at the cell corners where the walls of three or more spermatids meet each other (Fig. 4d) and where the corners contact the inner antheridial walls (Fig. 4e). During deposition of callose, the development of the locomotory apparatus, including the multilayered structure (MLS) and basal bodies begins, and cytoplasmic bridges are visible between pairs of spermatids (Fig. 4f, g). The wall produced during cytokinesis (W1) progressively disintegrates but often remains visible as an amorphous region at the juncture of three or more spermatids (Fig. 4d) or as thin electron-dense boundaries between pairs of spermatids (Fig. 4f). Unlike during antheridial development, W1 no longer contains callose (Fig. 4c, d).

Following deposition of the thick uneven callosic wall (W3), spermatids lay down an evenly thin wall (W4) that averages 0.38 µm in thickness (Fig. 5a–d). When fixed in glutaraldehyde and manually released from antheridia, spermatid walls at this stage of development fluoresce intensely when stained with calcofluor white (Fig. 5a). When probed with the cellulose (Fig. 5b) and xyloglucan (Fig. 5c) MAbs, the gold labels are sparsely distributed along the wall. In contrast, galactoxyloglucan epitopes (labeled with LM25) are abundantly distributed

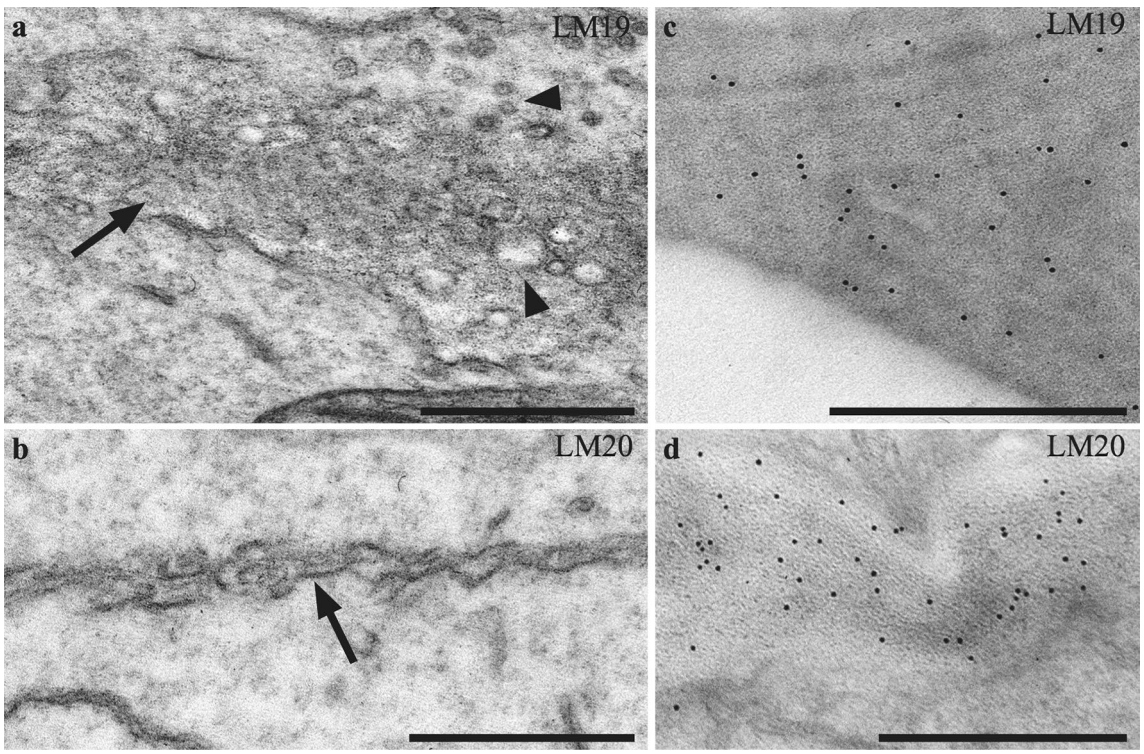

Fig. 3 Walls of antheridia and dividing spermatogenous cells immunogold labeled with LM19 and LM20 MAbs for HG pectins. **a** Forming wall (W1) (*arrow*) showing active vesicle deposition (*arrowheads*) at the cell plate. Unesterified HG epitopes are not detected with the LM19 MAb. **b** Likewise, methyl-esterified HG epitopes are not localized in the thin walls (*arrow*) using the LM20 MAb. **c**, **d** The antheridial walls are rich in both unesterified and methyl-esterified HG pectin epitopes. **c** LM19 epitopes are abundant and randomly distributed throughout the epidermal walls of the jacket cells. **d** Likewise, LM20 epitope localizations display a similar pattern in the inner jacket cell walls. *Scale bars*: 500 nm for **a**–**d**

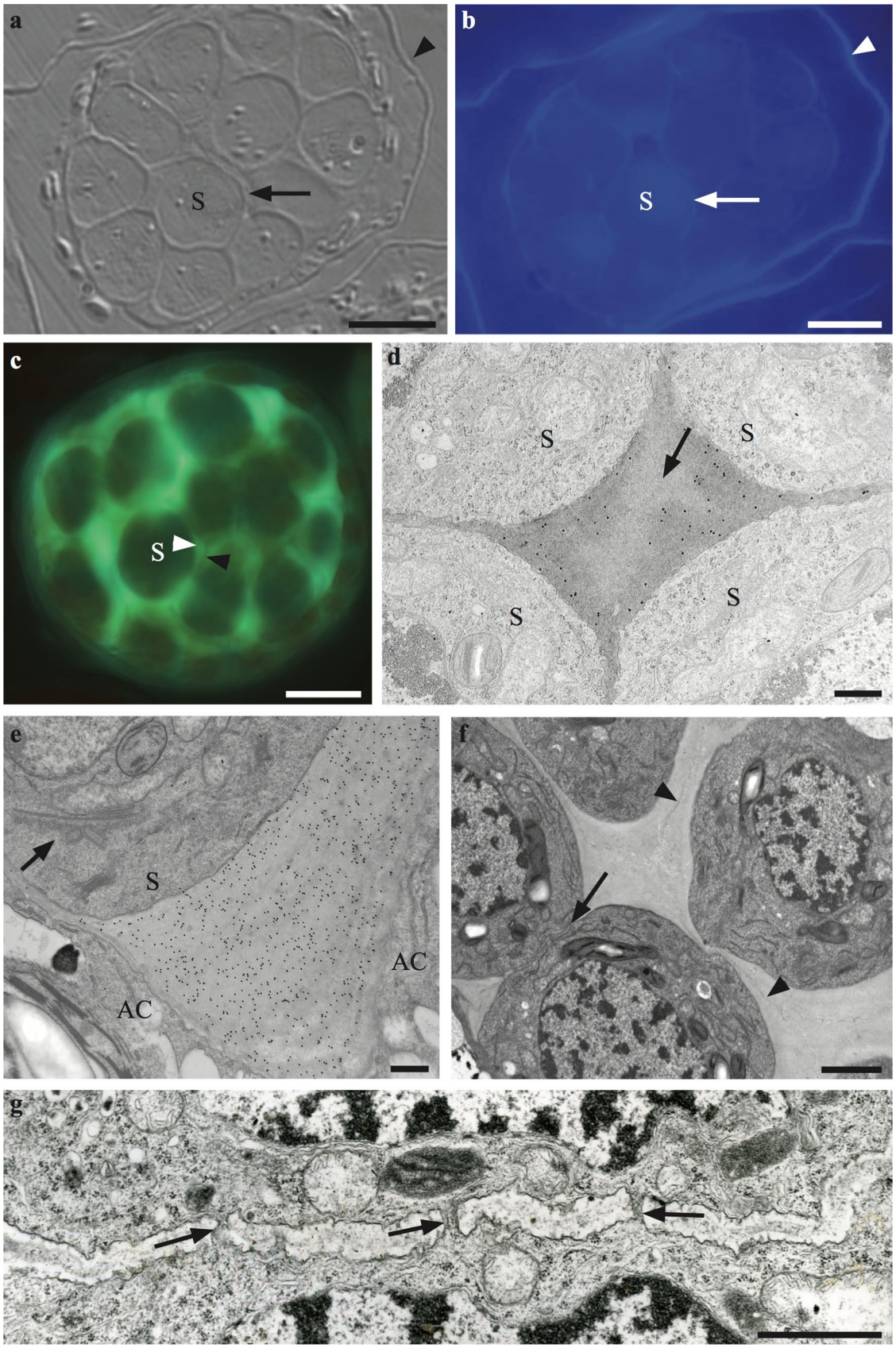
a
S
b
S
c
S
d
S
S
S
S
e
S
AC
AC
f
g

◂**Fig. 4** Young spermatid cell walls (W2 and W3). **a** DIC micrograph of young spermatids (*S*) with primary (W2) and newly forming secondary walls (W3) (*arrow*) in antheridium (*arrowhead*) after the final spermatogenous division. **b** The same section stained with calcofluor white illustrates that cellulose/hemicelluloses are more abundant in the newly formed spermatid (*S*) primary walls (W2) (*arrow*), albeit they faintly fluoresce compared to walls of the jacket cells (*arrowhead*). **c** An antheridium containing 32 spermatids (*S*) stained with aniline blue. Callose walls (W3) (*white arrowhead*), deposited inside of thin primary spermatid walls (W2) (*black arrowhead*), are thickest at the cell corners where three or more spermatids meet and thinner on the long walls between cells. **d** Immnuogold-labeled TEM micrograph probed with anti-callose antibody showing callose deposited at the corners and long walls between spermatids (*S*) but absent from the original primary cell wall (W2) (*arrow*). **e** Anti-callose labeling is abundant in the corners where spermatids (*S*) meet the antheridial cell walls (*AC*). **f** TEM of a control grid (i.e., was not exposed to a primary antibody) showing spermatids at the same developmental stage as shown in **a** and **b**. The *arrowheads* point to the spermatid primary walls (W2) that do not fluoresce in **c**. Cytoplasmic bridges persist between spermatids (*arrow*). **g** High magnification of the cytoplasmic bridges (*arrows*). *Scale bars*: 10 µm for **a**, **b**, and **c**; 500 nm for **d**, **e**; and **g**; 2 µm for **f**

throughout W4 (Fig. 5d). This wall does not bind to mannan and glucuronoxylan MAbs (data not shown).

In the final stages of sperm cell differentiation, W4 thickens irregularly and increases in density as an extensive extraprotoplasmic matrix (W5) forms between the gamete and the plasmalemma (Fig. 6a–c). It is within W5 that the sperm cell ultimately assumes its coiled configuration and the multiple flagella elongate. Essential to this process is elimination of excess cytoplasm and progressive separation of the nearly four coils of the mature gamete. The nucleus has initiated condensation and is elongated and coiled around the centrally positioned mass of cytoplasm (Fig. 6a). By this stage of differentiation, the spline and the locomotory apparatus, including flagella, are formed (Fig. 6b). The specific binding ß-D-glucosyl Yariv (ßGlucY) in W5 is striking and well illustrates the abundance of arabinogalactan proteins (AGPs) in the extraprotoplasmic matrix (Fig. 6c). No cellulose or hemicellulose epitopes are labeled in W5 with the CMB3a, LM15 and LM25 MAbs. As spermatids continue to develop, the callosic wall (W3) progressively disintegrates (Fig. 5a).

HG pectins as detected with the LM19 (Fig. 6d) and LM20 (Fig. 6e) MAbs are not present during any stage of spermatid development. For a comparison, the inner walls of the antheridial jacket cells are included to illustrate the abundant labeling of unesterified (Fig. 6f) and methyl-esterified (Fig. 6g) pectins. Epitope localization and abundance in the walls of spermatogenous cells (W1) and spermatids (W2–W5) in *C. richardii* are summarized in Tables 2 and 3, respectively.

Discussion

The process of spermatogenesis in plants with motile gametes involves the production of a series of unique cell walls that are integral to sperm cell differentiation and release. In *Ceratopteris*, five walls are made in sequence and each has a unique composition and function. The first wall (W1) separating dividing spermatogenous cells contains abundant callose and sparse hemicelluloses. Once formed, the cells that differentiate into motile gametes (spermatids) lay down four walls in sequence: W2, a thin cellulose and hemicellulose wall after the final cytokinesis; W3, a thick uneven callosic wall; W4, a thin cellulose plus hemicellulose wall; and W5, an AGP-rich matrix in which flagella elongate and the gamete changes shape (Lopez and Renzaglia 2014). To our knowledge, this is the most elaborate series of special cell walls involved in the development of any cell in land plants. Gametes are released in a thin porous wall, the so-called sperm "vesicle" that originates from W4, but they emerge from this wall when motile, becoming the only naked cell in the plant life cycle. This vesicle is of simple construction consisting solely of cellulose microfibrils crosslinked with xylan-containing hemicelluloses.

Callose is an abundant polysaccharide in two of the five walls involved in spermatogenesis in *Ceratopteris*. This polysaccharide is the major component detected in W1 during the proliferation of spermatogenous tissue, although trace amounts of hemicelluloses are present. Because callose is a linear polymer that does not form crystalline associations with neighboring strands, callosic matrices have a fluid-like nature (Nickle and Meinke 1998), a property that is desirable in rapidly dividing cells such as spermatogenous cells. The presence of callose in forming cell plates of seed plants is well documented (Samuels et al. 1995; Staehelin and Hepler 1996; Otegui and Staehelin 2000, 2004; Verma 2001). As a cell plate forms, it is enriched with pectins and callose but contains little if any cellulose (Moore and Staehalin 1988; Samuels et al. 1995; Otegui and Staehelin 2000) but as the plate matures, callose is slowly degraded by β-1,3-glucanase and replaced by cellulose and other wall components (Samuels et al. 1995; Verma 2001). Callose and hemicelluloses are deposited in cell plates during spermatogenesis in *Ceratopteris*, as in other plant cells but cellulose is sparse to lacking and pectins are absent.

It is the fifth and final mitotic division of the spermatogenous cells that produces male gametes. Cell walls produced following this division (W2) are extremely thin and transient as callose quickly disappears and is replaced by a network of calcofluor-binding polymers. Straightaway and in unison, spermatids deposit a thick wall of callose (W3) between the plasmalemma and W2. Owing to its physical properties (non-crystalline with limited and selective permeability), this callose stage of sperm cell development may also serve

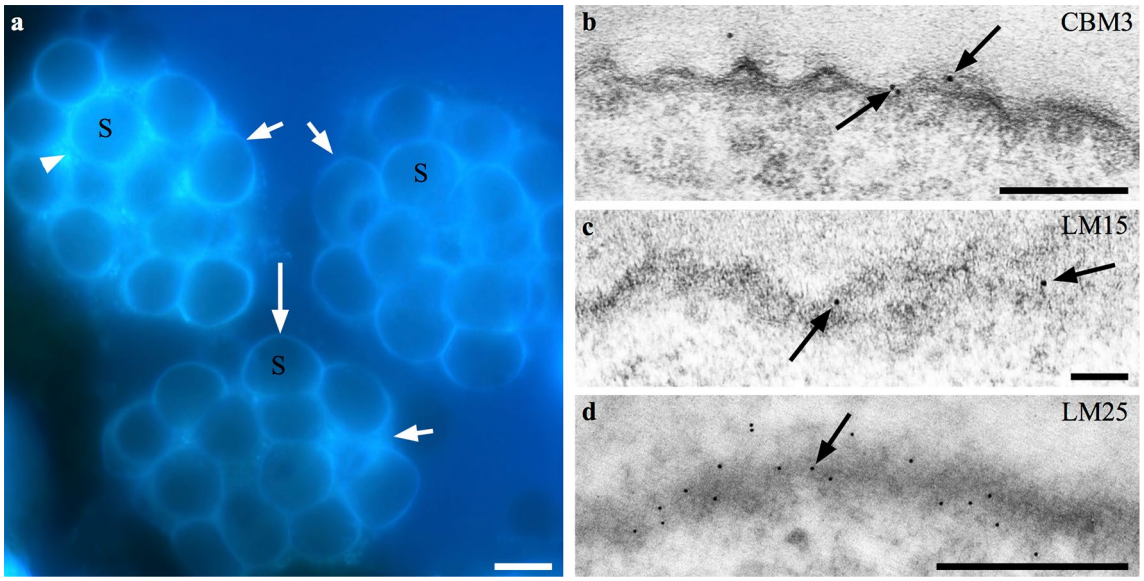

Fig. 5 Midstage spermatids (W2, W3, W4). **a** Spermatids (*S*) fixed in 2% glutaraldehyde are pushed out of antheridia in clusters of rounded cells (*short arrows*). The fourth wall layer (W4) (*long arrow*) surrounding sperm cells (*S*) fluoresces intensely for cellulose/hemicellulose when double stained with calcofluor and aniline blue. Degradation of the callose wall (W3) has begun (*arrowhead*). **b** The binding of the cellulose probe, CMB3a, to W4 is weak and labels are unevenly distributed (*arrows*). **c** Similarly, the binding of xyloglucan epitopes (*arrows*) to the LM15 MAb is weak and the gold particles are randomly distributed along this wall layer. **d** In contrast, copious galactoxyloglucan epitopes (*arrow*) were localized with the LM25 MAb. *Scale bars* 10 µm for **a**; 500 nm for **b** and **d**; 100 nm for **c**

to protect these cells from pathogens and fungal attack as speculated in other callose-eliciting responses (Kim et al. 2005; Jacobs et al. 2003; Nishimura et al. 2003; Flors et al. 2005; El Hadrami et al. 2010; Luna et al. 2011; Zimmerli et al. 2004; Koh et al. 2012; Ellinger et al. 2013; Eggert et al. 2014). Additionally, callose has a high water-holding capacity (Bhalla and Slattery 1984) that may provide essential protection from desiccation, low temperatures, and heavy metals for vulnerable developing gametes (Kartusch 2003; Krzeslowska 2011; Piršelová and Matušíková 2013). In desiccation-adapted green algae, callose in the cell walls provides the flexibility to shrink and expand as they dry and rehydrate (Herburger et al. 2015).

The thick callosic layer in W3 of *Ceratopteris* is found in other ferns and in liverwort tissues (Gorska-Brylass 1969, 1970; Cave and Bell 1973; Gori et al. 1997; Muccifora and Bellani 2011; Kotenko 1990). Our survey of callose across monilophytes indicates that a callose stage characterizes even the early divergent eusporangiate taxa (e.g., *Botrychium*) and is integral to spermatogenesis (Renzaglia and Lopez unpublished). During microgametogenesis in pollen, the generative cell becomes completely isolated from the vegetative cell cytoplasm by the formation of a callose wall devoid of plasmodesmata or cytoplasmic connections (Hepslop-Harrison 1968; Gorska-Brylas 1968, 1970; Kuhn and Mariath 2014). It is reasonable to speculate that the callose associated with antheridial development in monilophytes was co-opted and modified for microsporogenesis in gymnosperms and later in angiosperms. The putative callose synthase genes involved in pollen development, GSL-10 and GSL-8 (Cals9 and Cals10) are critical for male gametogenesis in *Arabidopsis* (Töller et al. 2008; Huang et al. 2009; Piršelová, Matušíková 2013). Examination of *gsl8* and *gsl10* mutant pollen revealed abnormal division patterns during mitosis, irregular deposition of callose and generative cells that failed to migrate into the vegetative cytoplasm (Töller et al. 2008). These two genes are the likely candidates for the synthesis of callose associated with male gametes in *Ceratopteris*.

Following callose deposition, young spermatids produce a wall layer (W4) of cellulose microfibrils that are extensively crosslinked to hemicelluloses and completely free of pectin polymers. Deposition of this wall layer severs the cytoplasmic connections between gametes. Although thin and loosely constructed, this wall functions to: (1) isolate individual spermatids, (2) provide a semirigid structure that borders the differentiating gamete and the matrix (W5) in which it is embedded, and (3) encapsulate and protect newly released spermatozoids as they initiate motility. Wall 5 is a matrix that is enriched in AGPs but is devoid of other wall polysaccharides. Within the matrix of W5, gametes undergo their metamorphosis to produce 70 plus flagella, eliminate cytoplasm and undergo dramatic shape changes (Lopez and Renzaglia 2014). During these processes, the primary spermatid wall (W2) disintegrates, the callosic wall (W3) progressively disappears, and the AGP matrix (W5) dissolves,

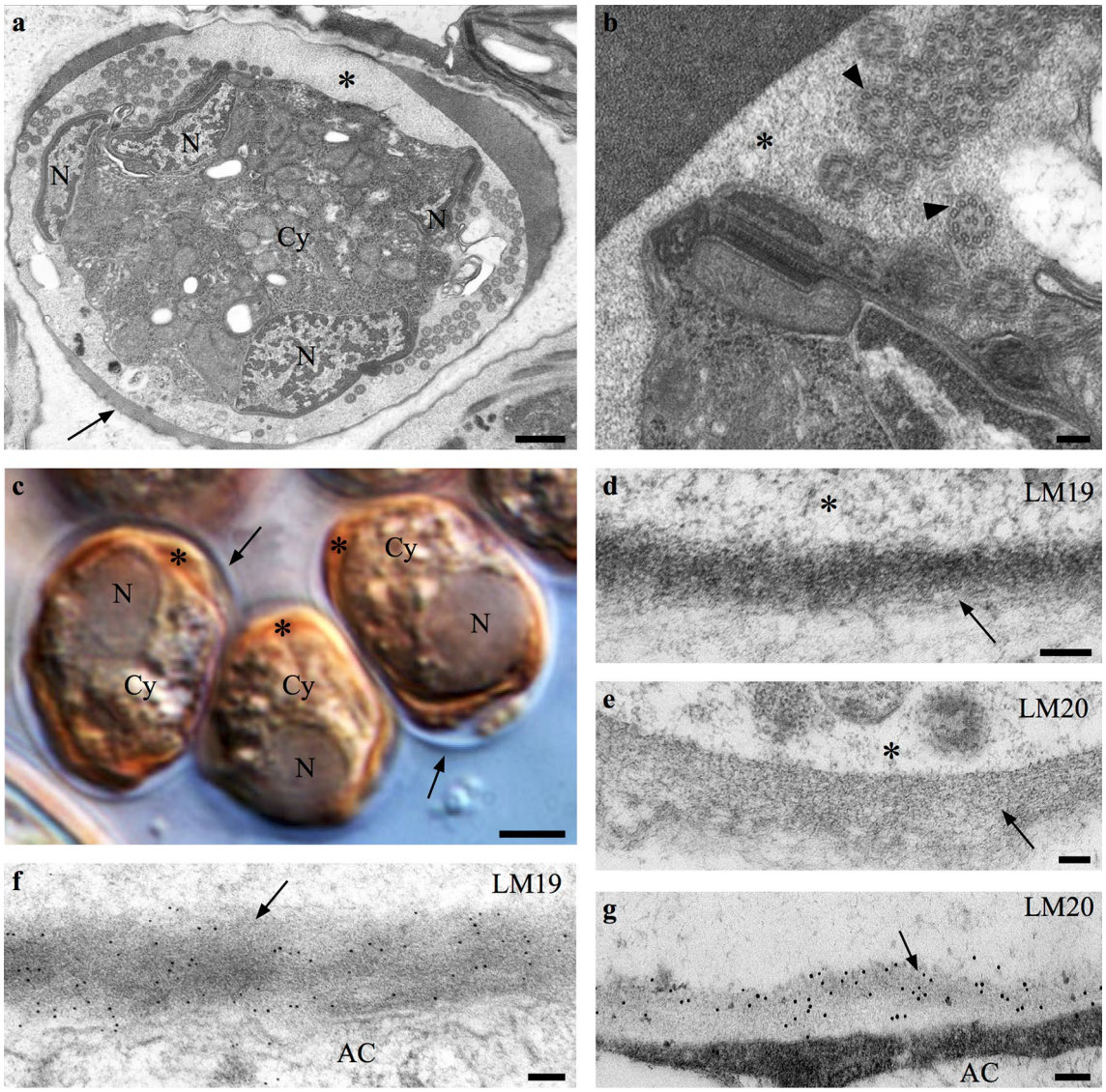

Fig. 6 Spermatid walls (W4 and W5) examined for the presence of pectin and AGP epitopes. **a** TEM showing a late midstage spermatid completely embedded in the fully formed fifth wall layer called the extraprotoplasmic matrix (*asterisk*). W4 (*arrow*) at this stage appears dense and unevenly thickened. Nuclear (*N*) coiling has begun around the mass of centrally positioned cytoplasm (*Cy*) and flagellar development is complete. **b** Higher magnification of W5 (*asterisk*) reveals the fibrillar nature of the extraprotoplasmic matrix and the extent to which this wall completely encompasses the spermatid as the 70 + flagella (*arrowheads*) elongate and the cell takes on a coiled architecture. **c** DIC micrograph of young spermatids manually released from the antheridium and treated with the Yariv reagent ß-glucosyl (ßGlucY) for AGPs. The red stain in W5 (*asterisk*) illustrates the abundance of AGPs in this wall. In contrast, W4 (*arrows*) did not bind to the ßGlucY. The nucleus (*N*) at this stage of development is no longer centrally positioned in the cytoplasm (*Cy*). **d**–**g** Immunogold localizations using pectin MAbs. **d** There is no binding of unesterified HG in W4 (*arrow*) or in W5 (*asterisk*) with the LM19 MAb. **e** W4 (*arrow*) and W5 (*asterisk*) also lack methyl-esterified pectin epitopes as there is no binding of gold particles using the LM20 MAb. **f**, **g** The inner wall layer of antheridial cells (*AC*) is included to illustrate the strong binding of the LM19 MAb (*arrow*) in **f** and the LM20 MAb (*arrow*) in **g** indicating the presence of unesterified HG and methyl-esterified HG pectins, respectively. *Scale bars*: 500 nm for **a**; 100 nm for **b** and **d**–**g**; 10 µm for **c**

leaving only the thin cellulose and hemicellulose wall (W4) surrounding the naked, mature spermatozoid.

Like spermatogenous, oogenesis in *Ceratopteris* involves the deposition of specialized matrices that are involved in egg maturation and fertilization (Lopez and Renzaglia 2016). Firstly, nascent eggs are isolated from their primary walls and the surrounding gametophyte tissue by the formation of a thick AGP-filled matrix expressing (1,5)-α-L-arabinan epitopes. Secondly, as the first matrix forms, the egg deposits an additional membranous matrix, the egg envelope, at the cell periphery that is rich in both AGPs and arabinan pectins. Recent studies have shown that arabinose-rich

Table 2 Relative intensity of immunogold labeling and histochemical staining of the walls of spermatogenous cells with aniline blue, calcofluor white and the following monoclonal antibodies (MAbs) anti-callose, CBM3a, LM15, LM21, LM25, LM28, LM19 and LM20

MAbs	Spermatogenous walls (W1)
Aniline blue	+++
Calcofluor white	−
Anti-callose	+++
CBM3a (cellulose)	+
LM15 (xyloglucan)	++
LM21 (mannan)	−
LM25 (galactoxyloglucan)	+
LM28 (glucuronoxylan)	−
LM19 (unesterified HG)	−
LM20 (esterified HG)	−

+++, Very strong; ++, strong; +, weak; −, absent

Table 3 Relative intensity of histochemical staining and immunogold labeling with nine MAbs of the four cell walls during sperm cell differentiation following the formation of primary walls (W1) in the antheridium

Stains and MAbs	Spermatid walls			
	W2	W3	W4	W5
Aniline blue	−	+++	−	−
Calcofluor white	+	−	++	−
Yariv ßGluc	−	−	−	+++
Anti-callose	−	+++	−	−
CBM3a (cellulose)	±	−	+	−
LM15 (xyloglucan)	±	−	+	−
LM21 (mannan)	−	−	−	−
LM25 (galactoxyloglucans)	±	_	+++	−
LM28 (glucuronoxylans)	−	−	−	−
LM19 (unesterified HG)	−	−	−	−
LM20 (esterified HG)	−	−	−	−

+++, very strong; ++, strong; +, weak; −, absent; ±, weak/absent

polymers provide a high degree of flexibility and plasticity to plant cell walls (Jones et al. 2003; Ulvskov et al. 2005; Verhertbruggen and Knox 2007; Gomez et al. 2009; Moore et al. 2013). Developing male gametes, unlike egg cells, do not produce pectinaceous walls. Egg cells, in turn, lack callose, cellulose and hemicellulose matrices during differentiation (Lopez and Renzaglia 2016). An important similarity between male and female gamete development in *Ceratopteris* is that AGPs are abundant, albeit AGP epitopes are differentially expressed and vary between the two processes (Lopez and Renzaglia 2014, 2016).

Now that the sequence and composition of special walls associated with spermatogenesis and oogenesis have been elucidated in a leptosporangiate fern, it is pertinent to examine the same processes in representatives from other seed-free plant groups. For example, it has been shown that the thick walls of spermatogenous cells in mosses react strongly to the periodic acid Schiff's (PAS) stain for pectic polysaccharides and are readily digested by hemicellulase and pectinase (Vian 1970). These findings indicate that unlike in *Ceratopteris*, pectins and hemicellulose are present around young spermatids of mosses. Whether callose is also there remains to be examined.

Today, we have an ever-increasing array of monoclonal antibodies at our disposal to characterize many of the components found in plant cell walls. It would be a worthy undertaking to continue immunolocalization studies of cell walls across the diversity and life history of seed-free land plants. Wall ontogeny during specialized but essential processes such as gametogenesis, sporogenesis and embryogenesis provides a glimpse at how early land plants utilized the array of cell wall polymers in their evolutionary toolbox.

Author contribution statement RAL designed the study, performed the immunolocalizations and collected the data. RAL and KSR analyzed the data and prepared the manuscript.

Acknowledgements This work was supported by Grants from the National Science Foundation (DEB-0521177, DEB-06387622, DUE-1136414) and the National Institutes of Health (4R25GM107760-04). We also thank Dr. Les Hickok for graciously supplying the *Ceratopteris* spores used in this investigation.

References

Bhalla PL, Slattery HD (1984) Callose deposits make clover seeds impermeable to water. Ann Bot-Lond 53:125–128

Blake AW, McCartney L, Flint JE, Bolam DN, Boraston AB, Gilbert HJ, Knox JP (2006) Understanding the biological rational for the diversity of cellulose-directed carbohydrate-binding modules in prokaryotic enzymes. J Biol Chem 281:29321–29329

Buchanan BB, Gruissem W, Jones RL (eds) (2000) Biochemistry and molecular biology of plants. Wiley, London

Burgert I, Fratzl P (2009) Plants control the properties and actuation of their organs through the orientation of cellulose fibrils in their cell walls. Integr Comp Biol 49:69–79

Cave CF, Bell PR (1973) The cytochemistry of the walls of the spermatocytes of *Ceratopteris thalictroides*. Planta 109:99–104

Cornuault V, Buffetto F, Rydahl MG, Marcus SE, Torode TA, Xue J, Crépeau MJ, Faria-Blanc N, Willats WG, Dupree P, et al. (2015) Monoclonal antibodies indicate low-abundance links between heteroxylan and other glycans of plant cell walls. Planta 242:1321–1334

Eggert D, Naumann M, Reimer R, Voigt CA (2014) Nanoscale glucan polymer network causes pathogen resistance. Sci Rep-UK 4:4159

El Hadrami A, Adam LR, El Hadrami I, Daayf F (2010) Chitosan in plant protection. Mar Drugs 8:968–987

Ellinger D, Naumann M, Falter C, Zwikowics C, Jamrow T, Manisseri C, Somerville SC, Voigt CA (2013) Elevated early callose deposition results in complete penetration resistance to powdery mildew in *Arabidopsis*. Plant Physiol 161:1433–1444

Evert R (2006) Esau's plant anatomy: meristems, cells and tissues—their structure, function, and development, 3rd edn. Wiley, New Jersey

Flors V, Ton J, Jakab G, Mauch-Mani B (2005) Abscisic acid and callose: team players in defence against pathogens? J Phytopathol 153:377–383

Gomez LD, Steele-King CG, Jones L, Foster JM, Vuttipongchaikij S, McQueen-Mason SJ (2009) Arabinan metabolism during seed development and germination in *Arabidopsis*. Mol Plant 2:966–976

Gori P, Muccifora S, Woo SL, Bellani LM (1997) An ultrastructural study of the mature spermatozoid of the fern *Asplenium trichomanes* L. subsp. trichomanes. Sex Plant Reprod 10:142–148

Gorska-Brylass A (1968) Callose in the cell walls of the developing male gametophyte in Gymnospermae. Acta Soc Bot Pol 37:119–124

Gorska-Brylass A (1969) Callose in gametogenesis in liverworts. Bull Pol Acad Sci Biol Sci 17:549–554

Górska-Brylass A (1970) The "callose stage" of the generative cells in pollen grains. Grana 10:21–30

Herburger K, Lewis LA, Holzinger A (2015) Photosynthetic efficiency, desiccation tolerance and ultrastructure in two phylogenetically distinct strains of alpine *Zygnema* sp. (Zygnematophyceae, Streptophyta): role of pre-akinete formation. Protoplasma 252:571–589

Heslop-Harrison J (1968) Synchronous pollen mitosis and the formation of the generative cell in massulate orchids. J Cell Sci 3:457–466

Huang L, Chen XY, Rim Y, Han X, Cho WK, Kim SW, Kim JY (2009) *Arabidopsis* glucan synthase-like 10 functions in male gametogenesis. J Plant Physiol 166:344–352

Jacobs AK, Lipka V, Burton RA, Panstruga R, Strizhov N, Schulze-Lefert P, Fincher GB (2003) An *Arabidopsis* callose synthase, GSL5, is required for wound and papillary callose formation. Plant Cell 15:250–313

Jones L, Milne JL, Ashford D, McQueen-Mason SJ (2003) Cell wall arabinan is essential for guard cell function. Proc Natl Acad Sci 100:11783–11788

Kartusch R (2003) On the mechanism of callose synthesis induction by metal ions in onion epidermal cells. Protoplasma 220:219–225

Kaźmierczak A (2008) Cell number, cell growth, antheridiogenesis, and callose amount is reduced and atrophy induced by deoxyglucose in *Anemia phyllitidis* gametophytes. Plant Cell Rep 27:813–821

Kim JY, Rim Y, Wang J, Jackson D (2005) A novel cell-to-cell trafficking assay indicates that the KNOX homeodomain is necessary and sufficient for intercellular protein and mRNA trafficking. Gene Dev 19:788–793

Knox JP (2008) Revealing the structural and functional diversity of plant cell walls. Curr Opin Plant Biol 11:308–313

Koh EJ, Zhou L, Williams DS, Park J, Ding N, Duan YP, Kang BH (2012) Callose deposition in the phloem plasmodesmata and inhibition of phloem transport in citrus leaves infected with *Candidatus Liberibacter asiaticus*. Protoplasma 249:687–697

Kotenko JL (1990) Spermatogenesis in a homosporous fern, *Onoclea sensibilis*. Am J Bot 77:809–825

Krzesłowska M (2011) The cell wall in plant cell response to trace metals: polysaccharide remodeling and its role in defense strategy. Acta Physiol Plant 33:35–51

Kuhn SA, de Araujo-Mariath JE (2014) Reproductive biology of the "Brazilian pine" (*Araucaria angustifolia*–Araucariaceae): development of microspores and microgametophytes. Flora 209:290–298

Lamport DT, Várnai P (2013) Periplasmic arabinogalactan glycoproteins act as a calcium capacitor that regulates plant growth and development. New Phytol 197:58–64

Lopez RA, Renzaglia KS (2014) Multiflagellated sperm cells of *Ceratopteris richardii* are bathed in arabinogalactan proteins throughout development. Am J Bot 101:2052–2061

Lopez RA, Renzaglia KS (2016) Arabinogalactan proteins and arabinan pectins abound in the specialized matrices surrounding female gametes of the fern *Ceratopteris richardii*. Planta 243:947–957

Luna E, Pastor V, Robert J, Flors V, Mauch-Mani B, Ton J (2011) Callose deposition: a multifaceted plant defense response. Mol Plant-Microbe In 24:183–193

Marcus SE, Blake AW, Benians TA, Lee KJ, Poyser C, Donaldson L, Leroux O, Rogowski A, Petersen HL, Boraston A, Gilbert HJ (2010) Restricted access of proteins to mannan polysaccharides in intact plant cell walls. Plant J 64:191–203

Marcus SE, Verhertbruggen Y, Hervé C, Ordaz-Ortiz JJ, Farkas V, Pedersen HL, Willats WG, Knox JP (2008) Pectic homogalacturonan masks abundant sets of xyloglucan epitopes in plant cell walls. BMC Plant Biol 8:60

McCabe PF, Levine A, Meijer PJ, Tapon NA, Pennell RI (1997) A programmed cell death pathway activated in carrot cells cultured at low cell density. Plant J 12:267–280

Meikle PJ, Bonig I, Hoogenraad NJ, Clarke AE, Stone BA (1991) The location of (1→ 3)-β-glucans in the walls of pollen tubes of Nicotiana alata using a (1→ 3)-β-glucan-specific monoclonal antibody. Planta 185:1–8

Moore PJ, Staehelin LA (1988) Immunogold localization of the cell-wall-matrix polysaccharides rhamnogalacturonan I and xyloglucan during cell expansion and cytokinesis in *Trifolium pratense* L.; implication for secretory pathways. Planta 174:433–445

Moore JP, Nguema-Ona EE, Vicré-Gibouin M, Sørensen I, Willats WG, Driouich A, Farrant JM (2013) Arabinose-rich polymers as an evolutionary strategy to plasticize resurrection plant cell walls against desiccation. Planta 237:739–754

Muccifora S, Bellani LM (2011) Antheridial dehiscence in ferns. Plant Syst Evol 297:51–56

Nickle TC, Meinke DW (1998) A cytokinesis-defective mutant of Arabidopsis (cyt1) characterized by embryonic lethality, incomplete cell walls, and excessive callose accumulation. Plant J 15:321–332

Nishimura MT, Stein M, Hou BH, Vogel JP, Edwards H, Somerville SC (2003) Loss of a callose synthase results in salicylic acid-dependent disease resistance. Science 301:969–972

Otegui M, Staehelin LA (2000) Cytokinesis in flowering plants: more than one way to divide a cell. Curr Opin Plant Biol 3:493–502

Otegui MS, Staehelin LA (2004) Electron tomographic analysis of post-meiotic cytokinesis during pollen development in *Arabidopsis thaliana*. Planta 218:501–515

Pedersen HL, Fangel JU, McCleary B, Ruzanski C, Rydahl MG, Ralet MC, Farkas V, von Schantz L, Marcus SE, Andersen MC, Field R (2012) Versatile high resolution oligosaccharide microarrays for plant glycobiology and cell wall research. J Biol Chem 287:39429–39438

Piršelová B, Matušíková I (2013) Callose: the plant cell wall polysaccharide with multiple biological functions. Acta Physiol Plant 35:635–644

Renzaglia KS, Garbary DJ (2001) Motile male gametes of land plants: diversity, development, and evolution. Crit Rev Plant Sci 20:107–213

Rudall PJ, Bateman RM (2007) Developmental bases for key innovations in the seed-plant microgametophyte. Trends Plant Sci 12:317–326

Samuels AL, Giddings TH, Staehelin LA (1995) Cytokinesis in tobacco BY-2 and root tip cells: a new model of cell plate formation in higher plants. J Cell Biol 130:1345–1357

Staehelin LA, Hepler PK (1996) Cytokinesis in higher plants. Cell 84:821–824

Töller A, Brownfield L, Neu C, Twell D, Schulze-Lefert P (2008) Dual function of Arabidopsis glucan synthase-like genes GSL8 and GSL10 in male gametophyte development and plant growth. Plant J 54:911–923

Ton J, Mauch-Mani B (2004) β-amino-butyric acid-induced resistance against necrotrophic pathogens is based on ABA-dependent priming for callose. Plant J 38:119–130

Ulvskov P, Wium H, Bruce D, Jørgensen B, Qvist KB, Skjøt M, Hepworth D, Borkhardt B, Sørensen SO (2005) Biophysical consequences of remodeling the neutral side chains of rhamnogalacturonan I in tubers of transgenic potatoes. Planta 220:609–620

Verhertbruggen Y, Knox JP (2007) Pectic polysaccharides and expanding cell walls. In: Verbelen J-P, Vissenberg K (eds) Plant cell monographs: the expanding cell, vol 5. Springer, Berlin Heidelberg, pp 139–158

Verhertbruggen Y, Marcus SE, Haeger A, Ordaz-Ortiz JJ, Knox JP (2009) An extended set of monoclonal antibodies to pectic homogalacturonan. Carbohyd Res 344:1858–1862

Verma DP (2001) Cytokinesis and building of the cell plate in plants. Ann Rev Plant Biol 52:751–784

Vian B (1970) Observations sur l'evolution des substances intercellulaires pendant la spermatogénèse chez une hepatique, *Fossombronia angulosa*. Comptes Rendus de l'Académie des Sciences—Series D 270:1240–1243

Warne TR, Walker GL, Hickok LG (1986) A novel method for surface-sterilizing and sowing fern spores. Am Fern J 76:187–188

Wolf S, Hématy K, Höfte H (2012) Growth control and cell wall signaling in plants. Ann Rev Plant Biol 63:381–407

Yariv J, Lis H, Katchalski E (1967) Precipitation of Arabic acid and some seed polysaccharides by glycosyl phenylazo dyes. Biochem J 105:1c–2c

Zimmerli L, Stein M, Lipka V, Schulze-Lefert P, Somerville S (2004) Host and non-host pathogens elicit different jasmonate/ethylene responses in Arabidopsis. Plant J 40:633–646